Ab initio and hybrid density functional theory studies of the forward and reverse barriers for the $C_2H_4 + H \longrightarrow C_2H_5$ reaction

Branko S. Jursic

Department of Chemistry, University of New Orleans, New Orleans, Louisiana 70148, USA

Ab initio **and density functional theory (DFT) methods have been used to compute the potential energy surface of the $C_2H_4 + H \longrightarrow C_2H_5$ reaction. It was demonstrated that the computation of the forward reaction barrier is a very difficult problem. Even high level** *ab initio* **methods, such as MP2 and QCISD, had problems coming close to the experimental value. It was demonstrated that the G2 computational method predicts a very accurate energy profile for the reaction. DFT methods have a considerable problem in finding and optimizing the transition state structure. Many of these produced negative activation barriers. It was suggested that DFT methods overestimate the total energy of the hydrogen radical. Because of this effect, the heat of the reaction and the barrier of the reaction are too low. If this problem is solved, the energies generated by hybrid DFT methods for reactions which involve the hydrogen radical should be very close to experimental values.**

Introduction

One of our goals was to find a reliable computational method which would correctly reproduce reaction barriers. In this way, the experimental organic chemist could use these reliable computational techniques to assess reaction barriers for reactions which have not been studied experimentally. Presently, density functional theory (DFT) methods are becoming increasingly popular computational tools.[1] They are convenient cost-effective methods which incorporate an electron correlation into a calculation with a relatively straightforward, and in an essentially single-determinant, formalism which is modified by the Hartree–Fock technique. We have shown that hybrid DFT methods are very reliable for computing the activation barriers of cycloaddition,[2] rearrangement,[3] ring opening[4] and hydrogen abstraction[5] reactions. Other very accurate DFT methods failed to reproduce activation barriers for many of these reactions, especially ones which involve radicals.[6]

Rearrangement reactions are very important for the preparation of a wide variety of organic molecules.[7] Radical rearrangement reactions are usually not very selective and many chemists are interested in finding an accurate computational method which can handle these systems. We have demonstrated that the radical hydrogen abstraction reaction with relatively large organic molecules can be handled very well by DFT methods.[8] However, DFT methods have shown considerable problems when a very small molecule like hydrogen was used.[6] Keeping this in mind, we have chosen hydrogen radical elimination from the ethyl radical for our study. In addition to producing ethene as the model reaction for testing DFT methods, extensive experimental studies of the $C_2H_4 + H \longrightarrow C_2H_5$ reaction system are required.[9] Thus, the computed values can be compared with the experimental values. There are some *ab initio* studies that do not reproduce the experimental results with the desired accuracy.[10] Therefore, this system seems to be ideal for testing DFT methods and for computing activation barriers of radical rearrangement reactions.

Computational methodology

All calculations were performed with the GAUSSIAN 94 computational package.[11] Traditional Hartree–Fock (HF),[12] second-order Møller–Plesset energy correction (MP2);[13] and quadratic configuration interactions, singlet and doublet substitution with triples contribution to the energies [QCISD(T)][14] *ab initio* methods were used. The GAUSSIAN theoretical models (G1, G2 and G2MP2),[15] which are known to produce highly accurate energies were also used to compute the energies.

Three hybrid DFT methods were applied: Becke's three parameter functional[16] which has the form of $AE_x^{Slater} + (1 - A)E_x^{HF} + B\Delta E_x^{Becke} + E_c^{VWN} + C\Delta E_c^{non\text{-}local}$, where the non-local correlation is provided by the LYP[17] expression (B3LYP), Slater is provided by the Slater exchange functional,[18] and the constants A, B and C are those determined by Becke which fit into the G1[15] molecular set; Becke's three parameter functional,[16] B3LYP, in which the non-local correlation is provided by the Perdew 86 expression[19] (B3P86); and Becke's three parameter functional[16] in combination with a non-local correlation functional which is provided by the Perdew/Wang 91 expression[20] (B3PW91).

For all of the calculations, Gaussian type basis sets [3-21G, 6-31G(d), 6-311G(d,p); 6-311G(2d,2p)] were employed. The explanation and abbreviations of the basis sets are found in the GAUSSIAN computational package.[21] The transition state structure was found and optimized first with the AM1 MOPAC semiempirical method which was described previously.[22] Then, the obtained transition states were further optimized and verified through *ab initio* and DFT computations by performing the thermal and vibrational analyses described previously.[23]

Results and discussion

Using the results of the *ab initio* calculations, Hase and Schlegel[24] proposed a transition state model for the $C_2H_4 + H \longrightarrow C_2H_5$ reaction which appeared to fit all the available experimental data. The C_2H_5 dissociation and $C_2H_4 + H$ association thresholds are 38.0 and 2.5 kcal mol^{-1} (1 cal = 4.184 J), respectively, with a reaction enthalpy of 35.5 kcal mol^{-1}. The recently indicated problem which exists with DFT methods is in their ability to compute correctly activation energies for reactions that involve a hydrogen radical transfer.[6] Therefore, it is important to evaluate hybrid DFT methods on an example in which a hydrogen radical is added to a double bond.

The geometry of the transition state structure for the hydrogen radical addition to ethene is presented in Table 1. There are some interesting features of the transition state structure regarding different *ab initio* and DFT methods. The computed geometries of the transition state structure strongly depend on the method and basis set used. This can be expected for any

Table 1 The geometric parameters for the transition state structure when computed with *ab initio* and hybrid DFT methods

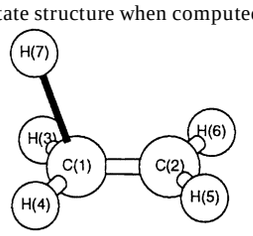

Theory model	*r*21/Å	*r*31/Å	*r*62/Å	*r*71/Å	*a*312/°	*a*621/°	*a*712/°	*d*7125/°
UHF/3-21G	1.354	1.073	1.073	2.017	121.3	121.6	106.0	86.4
UHF/6-31G(d)	1.359	1.075	1.075	2.004	121.2	121.5	106.3	86.8
UHF/6-311G(d,p)	1.357	1.075	1.075	1.983	121.1	121.4	106.6	86.6
UHF/6-311G(2d,2p)	1.352	1.073	1.073	1.981	121.1	121.4	106.4	86.6
MP2/6-31G(d)	1.339	1.084	1.084	1.903	121.1	121.6	107.5	88.1
MP2/6-311G(d,p)	1.333	1.084	1.084	1.867	121.1	121.4	107.2	88.3
MP2/6-311+G(2df,p)	1.327	1.082	1.082	1.842	121.2	121.5	107.1	88.9
QCISD/6-31G(d)	1.358	1.088	1.088	1.903	121.1	121.6	107.4	88.2
QCISD/6-311G(d,p)	1.353	1.087	1.087	1.976	121.1	121.4	106.7	88.7
B3LYP/6-31G(d)	1.337	1.087	1.087	2.330	121.8	121.8	104.2	89.5
B3LYP/6-311G(d,p)	1.335	1.084	1.085	2.238	121.7	121.7	104.9	89.4
B3LYP/6-311G(2d,2p)	1.331	1.082	1.082	2.237	121.6	121.6	105.0	89.5
B3PW91/3-21G	1.335	1.087	1.087	2.256	121.7	121.8	105.4	83.9
B3PW91/6-31G(d)	1.337	1.087	1.087	2.237	121.7	121.7	105.5	84.1
B3PW91/6-311G(d,p)	1.334	1.085	1.085	2.193	121.6	121.6	105.8	84.2
B3PW91/6-311G(2d,2p)	1.331	1.083	1.083	2.197	121.6	121.6	106.0	84.0

Table 2 The geometric parameters for the ethyl radical when computed with *ab initio* and hybrid DFT methods

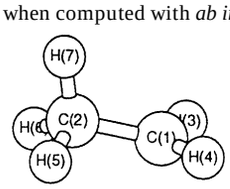

Theory model	*r*/21Å	*r*31/Å	*r*52/Å	*r*72/Å	*a*213/°	*a*125/°	*a*127/°	*d*7214/°
UHF/3-21G	1.507	1.073	1.084	1.089	120.4	111.1	111.3	85.0
UHF/6-31G(d)	1.498	1.075	1.086	1.091	120.4	111.4	111.8	82.5
UHF/6-311G(d,p)	1.498	1.076	1.086	1.091	120.4	111.3	111.6	82.6
UHF/6-311G(2d,2p)	1.495	1.073	1.083	1.088	120.4	111.3	111.6	82.6
MP2/6-31G(d)	1.498	1.082	1.093	1.100	120.7	111.4	111.9	82.9
MP2/6-311G(d,p)	1.492	1.082	1.093	1.099	120.5	111.4	111.6	82.6
MP2/6-311+G(2df,p)	1.482	1.079	1.091	1.097	120.9	111.7	111.7	82.7
QCISD/6-31G(d)	1.495	1.087	1.097	1.104	120.8	111.4	111.9	82.9
QCISD/6-311G(d,p)	1.499	1.086	1.096	1.103	120.5	111.3	111.6	82.6
B3LYP/3-21G	1.497	1.084	1.097	1.105	120.7	111.5	111.7	86.4
B3LYP/6-31G(d)	1.490	1.086	1.097	1.105	120.9	111.8	112.1	85.6
B3LYP/6-311G(d,p)	1.488	1.083	1.094	1.103	120.9	111.9	111.9	86.3
B3LYP/6-311G(2d,2p)	1.485	1.080	1.092	1.100	120.9	111.9	112.0	86.3
B3P86/3-21G	1.492	1.084	1.096	1.104	120.6	111.5	111.7	86.6
B3P86/6-31G(d)	1.484	1.085	1.096	1.104	120.9	111.8	112.1	85.9
B3P86/6-311G(d,p)	1.482	1.083	1.094	1.102	120.9	111.9	111.9	86.5
B3P86/6-311G(2d,2p)	1.479	1.082	1.091	1.099	120.9	111.9	112.0	86.4
B3PW91/3-21G	1.495	1.085	1.097	1.105	120.6	111.5	111.7	86.5
B3PW91/6-31G(d)	1.486	1.086	1.097	1.104	120.9	111.8	112.1	85.7
B3PW91/6-311G(d,p)	1.484	1.084	1.094	1.103	120.9	111.9	111.9	86.2
B3PW91/6-311G(2d,2p)	1.482	1.081	1.092	1.100	120.9	111.9	112.0	86.3

computed transition state structure. With HF, the newly forming C–H bond distance decreased slightly as the size of the basis set increased (Table 1). This distance was 2.017 Å with UHF/3-21G and 1.981 Å with UHF/6-311G(2d,2p). All other geometric parameters exhibited a lower basis set sensitivity. This agreement in the computed geometries is expected because the molecule is neutral and it is built only from carbon and hydrogen atoms. *Ab initio* methods with an electron correlation computed transition state structures with an even shorter C–H forming bond distances. Thus, MP2/6-311+G(2df,p) computed a C–H bond distance of 1.842 Å. Surprisingly, QCISD/6-311G(d,p) computed a transition state structure which is quite similar to the one generated by UHF/6-311G(d,p). In many of our computational studies, we have observed that QCISD generated transition state structures with much longer bonds of formation. It is important to point out that the transition state structures computed with the hybrid DFT methods have longer newly forming C–H bond distances than the transition state structures computed with the *ab initio* methods (Table 1). It is true that these bond distances decreased slightly with a larger basis set. Considering the geometries of the transition state structures, it can be stated that the hybrid DFT methods pre-

Table 3 The total energies (atomic units) of the molecular species involved in the $C_2H_4 + H \longrightarrow C_2H_5$ reaction

Theory model	$E_{C_2H_4}$/au	E_H/au	E_{TS}/au	$E_{C_2H_5}$/au
UHF/3-21G	−77.600 988	−0.496 199	−78.093 569	−78.163 646
UHF/6-31G(d)	−78.031 718	−0.498 233	−78.525 323	−78.597 149
UHF/6-311G(d,p)	−78.054 725	−0.499 810	−78.548 642	−78.619 745
UHF/6-311G(2d,2p)	−78.059 512	−0.499 810	−78.553 276	−78.624 399
UHF/6-311G(2d,2p) (0 K)	−78.005 378	−0.499 810	−78.498 704	−78.561 804
MP2/6-31G(d)	−78.294 283	−0.498 233	−78.772 966	−78.844 615
MP2/6-311G(d,p)	−78.381 583	−0.499 810	−78.864 751	−78.940 344
MP2/6-311+G(2df,p)	−78.425 307	−0.499 810	−78.908 650	−78.981 105
QCISD/6-31G(d)	−78.313 349	−0.498 233	−78.803 026	−78.869 044
QCISD/6-311G(d,p)	−78.372 910	−0.499 810	−78.866 987	−78.938 260
G1(0 K)	−78.414 012	−0.500 000	−78.908 493	−78.966 436
G1	−78.410 010	−0.497 639	−78.903 766	−78.961 501
G2(0 K)	−78.415 933	−0.500 000	−78.911 252	−78.970 168
G2	−78.411 931	−0.497 639	−78.906 524	−78.965 234
G2MP2(0 K)	−78.414 301	−0.500 000	−78.909 090	−78.968 121
G2MP2	−78.410 300	−0.497 639	−78.904 362	−78.963 186
B3LYP/6-31G(d)	−78.587 460	−0.500 273	−79.088 045	−79.157 868
B3LYP/6-311G(d,p)	−78.613 981	−0.512 156	−79.115 874	−79.183 653
B3LYP/6-311G(2d,2p)	−78.617 874	−0.512 156	−79.119 839	−79.187 658
B3LYP/6-311G(2d,2p)(0 K)	−78.566 912	−0.512 156	−79.067 849	−79.128 511
B3PW91/3-21G	−78.129 455	−0.486 068	−78.628 245	−78.699 946
B3PW91/6-31G(d)	−78.555 384	−0.486 960	−79.056 358	−79.129 104
B3PW91/6-311G(d,p)	−78.579 276	−0.478 939	−79.081 537	−79.152 418
B3PW91/6-311G(2d,2p)	−78.582 952	−0.478 939	−79.085 255	−79.156 183
B3PW91/6-311G(2d,2p)(0 K)	−78.531 989	−0.478 939	−79.033 241	−79.096 963

dicted earlier transition state structures when compared with the transition state structures computed with *ab initio* methods. Consequently, the predicted activation barriers for the hydrogen radical addition to ethene by hybrid DFT methods should be very low.

The *ab initio* computed structures of the ethyl radicals are very similar to each other. As seen in the case of the transition state computational studies, the bond distances generally decrease with a higher level of applied theory (Table 2). This observation is correct for both the *ab initio* and hybrid DFT computational methods. There are a couple of interesting points with regard to the ethyl radical. Although the symmetry was not restricted in the optimization of the geometry, all of the computed ethyl radical geometries had a plane of symmetry that went through the C(7)–C(2)–C(1) atoms. *Ab initio* and DFT methods consistently predicted that the ethyl radical was slightly pyramidal. A higher deviation from the planarity was computed with the *ab initio* methods. The dihedral angle predicted by the *ab initio* methods was *ca.* 82.5° (Table 2), while the hybrid DFT methods computed the angle to be 86.5°. The latter angle was much closer to the planarity radical and the d_{7214} of 90°. There are two possible structures for simple alkyl radicals.[25] They may have sp^2 bonding, in which case, the structure would be planar with the odd electron in a p orbital, or the bonding may be sp^3, which would make the structure pyramidal and place the odd electron in an sp^3 orbital. EPR spectra of CH_3 and other simple alkyl radicals, together with other evidence, indicate that alkyl radicals have a planar structure.[26] In addition, the electronic spectra of CH_3 and CD_3 radicals (generated by flash photolysis) in the gas phase definitely have established that radicals are planar or near-planar under these conditions.[27] The computed ethyl radical structures generated by the hybrid DFT methods are closer to planarity than the structures computed with the *ab initio* methods (Table 2).

The energies for the hydrogen radical addition to ethene are well known.[24] The total energies for reactants, transition state and product are summarized in Table 3. The computed activation barriers and enthalpies of the reaction are presented in Table 4. It is well known that accurate heats of reaction and barrier heights are more difficult to calculate directly than are the geometries.[28] The barrier height for the $H + C_2H_4$ addition was even more difficult to calculate accurately than for closed-shell chemical reactions. UHF *ab initio* methods usually suffer from spin contamination and cannot reproduce experimental reaction barriers. However, here it almost perfectly matches the experimental value of 2.5 kcal mol^{-1} (Table 4). We believe that this agreement was coincidental because, for many other reactions, the computed energies were quite different from the experimental values. For the transition state, the spin unrestricted MP2 also suffers from serious spin contamination problems and the barrier was about 8–10 kcal mol^{-1} higher than expected. Some of these problems were solved by using the less spin contamination affected QCISD *ab initio* method. With this method, the computed barriers were 1–3 kcal mol^{-1} higher than expected (Table 4). The problem of spin contamination was avoided by using the G1, G2 and G2MP2 computational approaches.[15] Indeed, these computational methods produced activation barriers that were *ca.* 2.5 kcal mol^{-1}.

There was a considerable problem in computing the transition state structure with the DFT methods. Our attempt to compute the transition state with BLYP, BP86 and BPW91 was unsuccessful. With Becke's three exchange functional, we had limited success. Two of these DFT methods were able to find transition state structures after continuous changes in the newly forming C–H bond distances. The procedure was tedious and time consuming. When obtained, the structures with the maximal energy were further optimized as previously described. With many of the DFT methods (B3P86, BLYP, BPW91 and BP86), the optimization does not lead to a transition state structure, but rather to the separated reactants. The location and optimization of the transition state structure with *ab initio* methods was a straightforward process. We have experienced the DFT optimization convergence problem in many previous cases and it was computationally very expensive to (keyword scf = qc) bring the optimization towards a minimum. In the optimization of the radical transition state structures, even this approach was not successful.

The computed activation barriers, with only two hybrid methods, are presented in Table 4. B3LYP with a modest basis set, such as 6-31G(d), estimated a negative activation barrier for

Table 4 The computed forward and reverse activation barriers and enthalpy for the $C_2H_4 + H \longrightarrow C_2H_5$ reaction[a]

Theory model	ΔE_I/kcal mol^{-1}	ΔE_{II}/kcal mol^{-1}	ΔE_{III}/kcal mol^{-1}
UHF/3-21G	2.3	44.0	−41.7
UHF/6-31G(d)	2.9	45.1	−42.2
UHF/6-311G(d,p)	3.7	44.6	−40.9
UHF/6-311G(2d,2p)	3.8	44.6	−40.8
UHF/6-311G(2d,2p)(0 K)	4.1	39.6	−35.5
MP2/6-31G(d)	12.3	45.0	−32.7
MP2/6-311G(d,p)	10.4	47.4	−37.0
MP2/6-311+G(2df,p)	10.3	45.5	−35.1
MP2/6-311+G(2df,p)(0 K)	12.1	41.6	−29.5
QCISD/6-31G(d)	5.4	41.4	−36.1
QCISD/6-311G(d,p)	3.6	44.7	−41.1
QCISD/6-311G(d,p)(0 K)	4.6	40.1	−35.5
G1(0 K)	3.5	36.4	−32.9
G1	2.4	36.2	−33.8
G2(0 K)	2.9	37.0	−34.0
G2	1.9	36.8	−34.9
G2MP2(0 K)	3.3	37.0	−33.7
G2MP2	2.2	36.9	−34.7
B3LYP/6-31G	−0.2	43.8	−44.0
B3LYP/6-311G(d,p)	0.2	42.5	−42.3
B3LYP/6-311G(2d,2p)	0.1	42.6	−42.5
B3LYP/6-311G(2d,2p)(0 K)	0.8	38.1	−37.3
B3PW91/3-21G	−8.0	45.0	−53.0
B3PW91/6-31G(d)	−8.8	45.6	−54.4
B3PW91/6-311G(d,p)	−14.6	44.5	−59.1
B3PW91/6-311G(2d,2p)	−14.6	44.5	−59.1
B3PW91/6-311G(2d,2p)(0 K)	−14.0	40.0	−54.0
Experimental	2.5	38.0	−35.5

[a] ΔE_I = forward reaction barrier; ΔE_{II} = reverse reaction barrier; ΔE_{III} = enthalpy of the reaction.

the hydrogen radical addition to ethylene. With a p orbital on the hydrogen, the computed activation barrier was in better agreement with the experimental value. A zero point energy correction does not substantially change the computed activation barrier (Table 4). The computed activation barrier with the B3PW91 hybrid DFT method was even worse. The estimated activation barrier was −8.0 to −14.6 kcal mol^{-1} (Table 4) depending on the basis set used. A zero point energy correction does not affect the barrier considerably. These two DFT methods are considered to be the most accurate of all the DFT methods currently available. They usually produce energies that are quite similar to the experimental values. In the case of the hydrogen radical addition to ethene, the computed geometries for the transition state structure and the ethyl radical are very similar. However, an evaluation of the activation barriers show that they differ by approximately 16 kcal mol^{-1}. We believe that this difference may come from a different treatment of the hydrogen radical because the reverse transition state has computed activation energies which are in close agreement with the experimental value.

Owing to the failure of other DFT methods to optimize the transition state structure, we cannot firmly state that they would also fail to reproduce correctly an experimental value for the activation barrier. If we compare the activation energies computed from the transition state structure obtained by the C–H new bond distance variation using BPW91 and BP86, the computed activation barrier should be *ca.* −16 kcal mol^{-1}. A similar approach was taken by Andzelm and co-workers when the hydrogen radical abstraction reaction with a hydroxyl radical was studied using DFT methods.[6]

The reaction barriers for the hydrogen elimination from the ethyl radical computed with *ab initio* methods were too high. It is interesting to point out that UHF/6-311G(2d,2p) with a zero point energy correction brings the computed activation barrier very close to the experimental value (Table 4). The difference was only 1.6 kcal mol^{-1}. This is actually a better value than those obtained with MP2 and QCISD. This finding was not expected based on the theory incorporated into these two computational methods. This was also true for the computed heats of reaction. The experimental value of −35.5 kcal mol^{-1} was excellently matched with the UHF/6-311G(2d,2p) (0 K) computed value of −35.5 kcal mol^{-1}. The reverse barrier (barrier for the hydrogen elimination from the ethyl radical) and heat of reaction was correctly estimated with the G2 computational model. This observation was expected knowing the high accuracy for energy computation which is obtained with this model.[15] An excellent activation barrier of 38.1 kcal mol^{-1} was computed with B3LYP/6-311G(2d,2p). In addition, an acceptable heat of reaction of −37.3 kcal mol^{-1} was also computed. We were able to obtain computational accuracy using these hybrid DFT methods for the activation barrier of many reactions.[2] The other hybrid DFT method predicted a slightly worse activation barrier (40 kcal mol^{-1}) and a very inaccurate heat of reaction which differed by 18.5 kcal mol^{-1} from the experimental values. These results are clearly not acceptable. These findings strongly establish that the total energy for the hydrogen radical was not computed correctly with DFT methods. We demonstrated our assumption by calculating the energy difference between the experimental and the B3PW91/3-6-311G(2d,2p) (0 K) computed activation barrier for the hydrogen addition to ethene. The difference was 16.5 kcal mol^{-1}. Subsequently, when this value was added to the computed heat of reaction, the estimated heat of reaction was then 37.5 kcal mol^{-1}. This was 2 kcal mol^{-1} higher than the experimental value. The same difference was obtained for the reverse activation barrier (Table 4). We believe that with properly corrected hybrid DFT methods, the total energy for the hydrogen radical can be accurately computed. Our results suggest that the major cause for the incorrect behaviour lies in the Slater exchange term of the DFT methods. The Becke's three exchange functional and BLYP correlation functional include a portion of the exact exchange, and B3LYP provides a much better description of the reaction profile than any other DFT method. Properly corrected DFT methods should be able to compute the potential energy surface for reactions which involve the hydrogen radical.

Conclusions

From the computed energy potential profile for the hydrogen radical addition to ethene, we can conclude that the computation of the forward reaction barrier was a surprisingly difficult process. The correlational *ab initio* method was a problem because it incorrectly estimated the experimental value. Only the suggested G1 and G2 *ab initio* methods correctly handled the hydrogen radical addition to alkenes. The computed energies are in excellent agreement with experiment values. Generally, DFT methods have an enormous difficulty in finding the transition state structure. For many DFT methods, a 'negative' activation barrier was computed by 'walking' reactants through the transition state through successive changes in the C–H newly forming bond distances. On the other hand, the experimental value for the reverse activation barrier (barrier for the hydrogen elimination from the ethyl radical) can be reproduced with hybrid DFT methods. The accuracy of the computed heat of reaction was in close correlation with the accuracy of the reaction barrier. The author believes, that the DFT methods showed a systematic problem when evaluating the energy of the free hydrogen radical, although, this problem was not mentioned in the paper by Pople and co-workers[6] for the $H_2 + H \longrightarrow H + H_2$ reaction or in the paper by Andzelm and co-workers for the $H_2O + H \longrightarrow HO + H_2$ reaction. The estimation of the activation barrier failed due to the incorrect DFT evaluation of the total energy for the hydrogen radical. If the evaluation of the total energy for the hydrogen radical is corrected, the activation barriers should be accurately computed by hybrid DFT methods.

References

1 *Density Functional Methods in Chemistry*, eds. J. Labanowski and J. Andzelm, Springer, Berlin, 1991; *Modern Density Functional Theory a Tool for Chemistry*, eds. J. M. Seminario and P. Politzer, Elsevier, New York, 1995; T. Ziegler, *Chem. Rev.*, 1991, **91**, 651.

2 B. S. Jursic and Z. Zdravkovski, *J. Chem. Soc., Perkin Trans. 2*, 1995, 1223; B. S. Jursic, *J. Mol. Struct.* (*THEOCHEM*), 1995, **358**, 139; B. S. Jursic, *J. Chem. Soc., Perkin Trans. 2*, 1996, 697; B. S. Jursic, *J. Mol. Struct.* (*THEOCHEM*), 1996, **365**, 55; B. S. Jursic, *J. Heterocycl. Chem.*, 1996, **33**, 1389.

3 B. S. Jursic, *Chem. Phys. Lett.*, 1996, **256**, 213; B. S. Jursic, *Int. J. Quant. Chem.*, in press; B. S. Jursic, *J. Mol. Struct.* (*THEOCHEM*), 1996, **366**, 109.

4 B. S. Jursic, *J. Mol. Struct.* (*THEOCHEM*), 1995, **357**, 243.

5 B. S. Jursic, *J. Chem. Phys.*, 1996, **104**, 4151; B. S. Jursic, *Chem. Phys. Lett.*, 1995, **244**, 263; B. S. Jursic, *J. Mol. Struct.* (*THEOCHEM*), 1996, **366**, 103; B. S. Jursic, *Chem. Phys. Lett.*, 1996, **256**, 603.

6 B. G. Johnson, C. A. Gonzalez, P. M. W. Gill and J. A. Pople, *Chem. Phys. Lett.*, 1995, **221**, 100; J. Baker, J. Andzelm, M. Muir and P. R. Taylor, *Chem. Phys. Lett.*, 1995, **237**, 531; B. S. Jursic, *Chem. Phys. Lett.*, in press.

7 P. de Mayo, *Rearrangements in Ground and Excited States*, 3 vols., Academic Press, New York, 1980; T. S. Stevens and W. E. Watts, *Selected Molecular Rearrangements*, Van Nostrand-Reinhold, Princeton, 1973.

8 B. S. Jursic, *J. Mol. Struct.* (*THEOCHEM*), in press.

9 Y. Feng, J. T. Niiranen, A. Benosura, V. D. Knyazev, D. Gutman and W. Tsang, *J. Phys. Chem.*, 1993, **97**, 871; P. D. Pacey and J. H. Wimalasen, *J. Phys. Chem.*, 1984, **88**, 5657; A. B. Trenwith, *J. Chem. Soc., Faraday Trans. 2*, 1986, **82**, 456; Y. Simmon, J. F. Foucaut and G. Scacchi, *Can. J. Chem.*, 1988, **66**, 2142.

10 W. L. Hase, H. B. Schlegel, V. Balbyshev and M. Page, *J. Phys. Chem.*, 1996, **100**, 5354.

11 GAUSSIAN94, Revision B.3, M. J. Frisch, G. W. Trucks, H. B. Schlegel, P. M. W. Gill, B. G. Johnson, M. A. Robb, J. R. Cheeseman, T. Keith, G. A. Petersson, J. A. Montgomery, K. Raghavachari, M. A. Al-Laham, V. G. Zakrzewski, J. V. Ortiz, J. B. Foresman, C. Y. Peng, P. Y. Ayala, W. Chen, M. W. Wong, J. L. Andres, E. S. Replogle, R. Gomperts, R. L. Martin, D. J. Fox, J. S. Binkley, D. J. Defrees, J. Baker, J. P. Stewart, M. Head-Gordon, C. Gonzalez and J. A. Pople, Gaussian, Inc., Pittsburgh, PA, 1995.

12 C. C. J. Roothan, *Rev. Mod. Phys.*, 1951, **23**, 69; J. A. Pople and R. K. Nesbet, *J. Chem. Phys.*, 1959, **22**, 571; R. McWeeny and G. Dierksen, *J. Chem. Phys.*, 1968, **49**, 4852.

13 C. Møller and M. S. Plesset, *Phys. Rev.*, 1934, **46**, 618; S. Saebo and J. Almlof, *Chem. Phys. Lett.*, 1989, **154**, 83; J. A. Pople, J. S. Binkley and R. Seeger, *Int. J. Quant. Chem. Symp.*, 1976, **10**, 1.

14 J. A. Pople, M. Head-Gordon and K. Raghavachari, *J. Chem. Phys.*, 1987, **87**, 5968.

15 J. A. Pople, M. Head-Gordon, D. J. Fox, K. Raghavachari and L. A. Curtiss, *J. Chem. Phys.*, 1989, **90**, 5622; L. A. Curtiss, C. Jones, G. W. Trucks, K. Raghavachari and J. A. Pople, *J. Chem. Phys.*, 1990, **93**, 2537; L. A. Curtiss, K. Raghavachari, G. W. Trucks and J. A. Pople, *J. Chem. Phys.*, 1991, **94**, 7221; L. A. Curtiss, K. Raghavachari and J. A. Pople, *J. Chem. Phys.*, 1993, **98**, 1293.

16 A. D. Becke, *J. Chem. Phys.*, 1993, **98**, 5648.

17 C. Lee, W. Yang and R. G. Parr, *Phys. Rev. B*, 1988, **37**, 785; B. Mielich, A. Savin, H. Stoll and H. Preuss, *Chem. Phys. Lett.*, 1989, **157**, 200.

18 J. C. Slater, *Quantum Theory of Molecular and Solids*, vol. 4, *The Self-Consistent Field for Molecular and Solids*, McGraw-Hill, New York, 1974.

19 J. P. Perdew, *Phys. Rev. B*, 1986, **33**, 8822; J. P. Perdew, *Phys. Rev. B*, 1987, **34**, 7046.

20 J. P. Perdew and Y. Wang, *Phys. Rev. B*, 1992, **45**, 13244.

21 M. J. Frisch, A. Frisch and J. B. Foresman, GAUSSIAN94 *User's Reference*, Gaussian, Inc., Pittsburgh, PA, 1995.

22 B. S. Jursic and Z. Zdravkovski, *J. Mol. Struct.* (*THEOCHEM*), 1994, **303**, 279.

23 B. S. Jursic, *J. Chem. Soc., Perkin Trans. 2*, 1996, 1021.

24 W. L. Hase and H. B. Schlegel, *J. Phys. Chem.*, 1982, **86**, 3901.

25 L. Kaplan, in J. K. Kochi, *Free Radicals*, Wiley, New York, 1973, vol. 2.

26 M. N. Paddon-Row and K. N. Houk, *J. Am. Chem. Soc.*, 1981, **103**, 5046 and references therein.

27 C. Yamada, K. Hirota and K. Kawaguchi, *J. Chem. Phys.*, 1981, **75**, 5256 and references therein.

28 W. J. Hehre, *Practical Strategies for Electronic Structure Calculations*, Wavefunction, Inc., Irvine, California, 1995.

Paper 6/03269I
Received 9*th May* 1996
Accepted 1*st November* 1996